Proceedings of the 1st Global Power and Propulsion Forum
GPPF 2017
Jan 16-18, 2014, Zurich, Switzerland
www.pps.global

GPPF-2017-47

APPLICATION OF PRESSURE- AND TEMPERATURE-SENSITIVE PAINT ON A HIGHLY LOADED TURBINE GUIDE VANE IN A TRANSONIC LINEAR CASCADE

Michael Hilfer
German Aerospace Center, DLR
Institute of Aerodynamics and Flow Technology
michael.hilfer@dlr.de
D-37073, Göttingen, Germany

Sebastian Dufhaus
RWTH Aachen University
Institute of Aerospace Systems
dufhaus@ilr.rwth-aachen.de
D-52062, Aachen, Germany

Anna Petersen
German Aerospace Center, DLR
Institute of Propulsion Technology
anna.petersen@dlr.de
D-37073, Göttingen, Germany

Daisuke Yorita
German Aerospace Center, DLR
Institute of Aerodynamics and Flow Technology
daisuke.yorita@dlr.de
D-37073, Göttingen, Germany

Christian Klein
German Aerospace Center, DLR
Institute of Aerodynamics and Flow Technology
christian.klein@dlr.de
D-37073, Göttingen, Germany

ABSTRACT

The transonic flow characteristics of highly loaded turbine guide vanes are complex. A typical transonic flow field deals with steady and unsteady shocks, separation bubbles and trailing edge shocks. This leads to further investigation of the shock wave-boundary layer interaction. To get a more detailed understanding of the flow characteristics a spatial pressure and temperature resolution on the blade surface is required.

Initially, steady pressure (PSP) and temperature (TSP) sensitive paints were applied to the suction side surface of a turbine guide vane in a transonic linear cascade (EGG) at DLR Göttingen. The qualitative and quantitative results agree well with results from Schlieren images and pressure taps taken.

Subsequently, in the same measurement campaign fast response Pressure Sensitive Paint (iPSP) was applied to the suction side of the guide vane. The qualitative data sets from the iPSP measurement are able to visualise unsteady flow characteristics in the cascade up to 1 kHz. Averaged iPSP results agree well with the pressure taps measurements taken at same conditions.

During this test campaign different flow characteristics including shocks, separation bubbles and laminar to turbulent boundary layer transition have been identified for different Mach numbers.

INTRODUCTION

Two important aspects in turbine design are the environmental and economic performance improvements. To achieve those goals it is necessary continuously to increase the understanding of the steady and unsteady flow characteristics in a turbine cascade. With increasing complexity of the flow in a turbine cascade, among others, due to addition of end wall and blade profiling, film cooling or vortex generators a spatial and temporal resolution of pressure and temperature on the surfaces is desired.

This work presents the experimental set up and the results of spatial measurement techniques (Pressure and Temperature Sensitive Paints) using paints recently developed by the German Aerospace Center (DLR), Institute of Aerodynamics and Flow Technology in collaboration with University Hohenheim and applied to a highly loaded turbine guide vane. This measurement technique provides steady and unsteady surface pressure distributions and steady temperature distribution for a typical flow field in the transonic turbine cascades which deals with oblique and normal shocks leading to the shock wave boundary layer interactions causing separation bubbles and laminar to turbulent boundary layer transitions. Especially the behaviour of the boundary layer was a topic of recent investigations Flaszynski et al. [1] and others. The recent advances in shock wave boundary layer interaction are also summarised by Gaitonde [2].

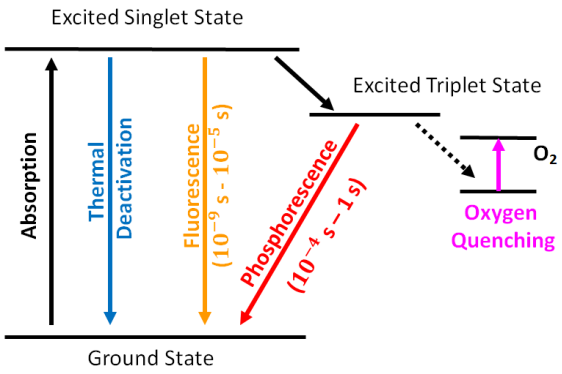

Figure 1: Simplified Jablonski Diagram, DLR PSP Course 2015, modified.

Pressure and Temperature Sensitive Paints (PSP and TSP) are mature optical pressure and temperature measurement techniques, which can provide a qualitative and quantitative surface pressure and temperature distribution over a model with a high spatial resolution. Additionally, fast response Pressure Sensitive Paints (iPSP) provide a temporally resolved surface pressure distribution resolving flow characteristics up to 10 kHz. Reviews of recent developments in fast response PSP technology are presented by Kameda [3] and Gregory et al. [4].

To detect the surface pressure discrete measurement techniques like pressure taps are commonly used in turbomachinery. Using such discrete techniques, expected flow phenomena have to be well considered beforehand and measurement positions fixed before the measurement. Spatial measurement techniques like PSP can avoid such considerations and can be used alongside the discrete techniques or as a standalone measurement technique.

Many flow phenomena on surfaces can also be visualised by two-dimensional sublimation techniques, Merzkirch [5]. In contrary to the PSP/TSP these kinds of techniques do not provide quantitative data.

Infrared imaging (IR) techniques are commonly used to detect laminar to turbulent transitions and separation bubbles, Bräunling [6] with high temperature resolution. Even though IR and TSP techniques are used to investigate same flow characteristics, in some cases, TSP is preferred due to hardware limitations of the IR techniques.

Schlieren images are often taken to understand the flow phenomena in a straight cascade, Bräunling [7]. Due to an optical effect, this technique can visualise flow field phenomena (shocks, separation bubbles) between two blades, whereas the PSP/TSP techniques always measure the flow on a surface. A combination of PSP/TSP with Schlieren imaging can provide flow field visualisation on the surface and across the flow.

Pressure tap data and Schlieren images recorded at the same flow conditions were used to validate the results from PSP/TSP/iPSP.

PSP/TSP MEASUREMENT METHODES

Two measurement methods, intensity and lifetime, were used during the tests.

Intensity Method

When the luminophore molecules, absorb light with a specific wavelength they are promoted to a higher energy state. These high energetic molecules can fall back to the ground state emitting light with a specific wavelength. The principle of PSP/TSP intensity method is based on the deactivation of the photochemical exited molecules in the presence of oxygen molecules or through thermal deactivation without radiation, i.e. quenching. The principle of this process is shown in the simplified Jablonski Diagram, Figure 1, and is well described by Liu and Sullivan [8].

For PSP the interaction of exited molecules with oxygen molecules increases the probability of the radiation-free process. Therefore, the higher the oxygen partial pressure on the surface of the paint, the lower the intensity emitted by the luminophores. For TSP the radiation-free process is caused by thermal deactivation of the exited molecule, hence lower intensity emitted with increasing temperature. In post processing, pressure and temperature information is obtained using pressure and temperature calibration data.

As described by Liu and Sullivan [8] it is possible to relate the spatial pressure *p* distribution to the intensity *I* ratio of the PSP luminescence at constant pressure condition *(ref)* during the test run *(run)* through Stern-Volmer Equation 1, where A and B are material coefficients, [8].

$$\frac{I_{ref}}{I_{run}} = A + B\frac{p_{run}}{p_{ref}} \qquad (1)$$

For the detection of the surface temperature the Arrhenius relation as shown in Equation 2 is used, [8].

$$ln\left[\frac{I(T_{run})}{I(T_{ref})}\right] = \frac{E_{nr}}{R}\left[\frac{1}{T_{run}} - \frac{1}{T_{ref}}\right] \qquad (2)$$

The luminescent intensity on the surface of the PSP/TSP is recorded with a digital camera (CCD or CMOS) equipped with an optical filter. Further description of the intensity method is presented by Liu and Sullivan [8]. The advantage of this method is its setup, where in its simplest form only one camera and one constant light source is needed. The disadvantages are possible errors from the model displacement during the test run and the need of wind-off images (images at known pressure and temperature conditions) for all model configurations, Liu and Sullivan [8].

Lifetime Method

The lifetime method relies on the pressure dependent luminescence decay after excitation light was turned off. The decay time is related to the surface pressures using modified Stern-Volmer Equation 3, [8].

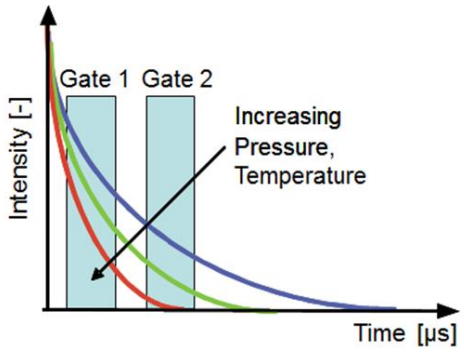

Figure 2: Timing Diagram of the Gated Intensity Ratio Method, Yorita et al. **[14]**, modified.

$$\frac{\tau_{ref}}{\tau_{run}} = A + B\frac{p_{run}}{p_{ref}} \qquad (3)$$

In this work, gated intensity ratio method is used, Figure 2, thereby a ratio of two pictures taken at a determined moment during luminescence decay time is a function of pressure or temperature, Equation 3. This lifetime method is further described by Yorita et al. [9].

$$f(p) = \frac{Gate\ 1}{Gate\ 2} \qquad (4)$$

The advantages of this method are its insensitivity to excitation intensity distribution, image registration error and camera pixel sensitivity. The disadvantages are the more complex setup compared to the intensity method with a need for a fast shutter camera and pulsed excitation light [9].

EXPERIMENTAL METHODS AND SET-UP

Wind Tunnel and Model

The experiments were performed in the transonic linear cascade wind tunnel at DLR Göttingen (EGG), Kost [10]. The wind tunnel was operated using dry air in a close loop, continuously driven by a 3 MW compressor stage. This air supply system enables an isentropic exit Mach number range from M = 0.5 to 1.3. The inlet turbulence level at the center of the flow is 0.4 %, Kapteijn et al. [11].

The investigated model is a highly loaded turbine guide vane, Figure 3, and was designed within the EC project TFAST (Transition location effect on shock wave boundary layer interaction) [12]. As shown in Figure 3, the blade was equipped with 20 pressure taps connected through 0.3 mm diameter tubing to miniature electronically scanned pressure module (ESP) and analogue-digital converter (Pressure Systems PSI 8400), Petersen [13]. The model is coated on the suction side surface and around the leading edge with the corresponding paint but only the area between x/c_{ax} = 0.60 and x/c_{ax} = 1.00 is visible to the measurement equipment.

In Figure 4 a sketch of the cascade with the positions of the camera and LED are shown. In Table 1 the cascade parameters are summarised.

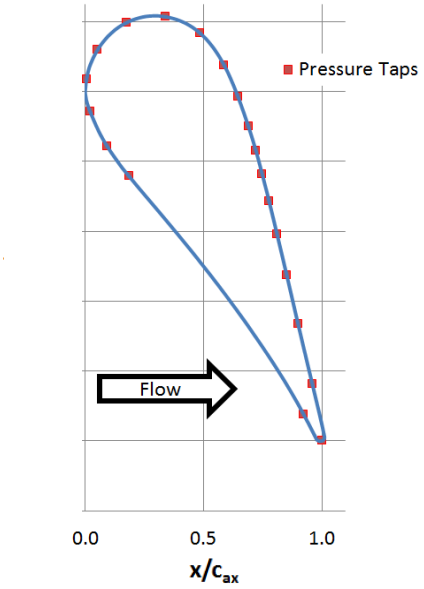

Figure 3: Nozzle guide vane with indicated pressure tap locations.

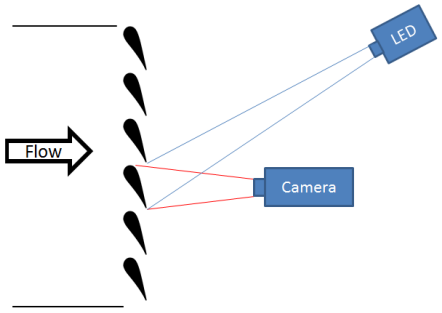

Figure 4: Sketch of the cascade with the position of the camera and LED.

Table 1: Cascade parameters

T_{in}	300 K
P_{in}	115 kPa
L_{in}	0.4 %
h/c	1.67
Pitch	68.2 mm
Throat	14.56 mm
Stagger angle	34.72 deg

Optical Instrumentation

For steady intensity and lifetime measurements, the high-resolution 14-bit CCD camera (PCO 4000, PCO) was used to record the luminescence. For unsteady measurements, a high-speed CMOS camera (FASTCAM SA 1.15, Photron) was used. Both cameras were operated with a Nikkor 35 mm f1.4 lens and an optical bandpass filter

(iPSP/PSP: LOT 650FS80, 630-710 nm >70%; TSP: LOT 630FS75, 595-665 nm >80%) to avoid collecting light from illumination. For the paint excitation, two UV LEDs (IL-106UV, HARDsoft) were used with a peak emission around 385 nm. A combination of a lens and a low pass optical filter with a cut-off wavelength around 550 nm was mounted in front of the LED to focus the light on the model as shown in Figure 4.

Calibration of PSP, TSP and iPSP

PSP/TSP and iPSP are lifetime or respectively intensity calibrated in an external calibration chamber at DLR Göttingen. The calibration system allows adjustment of pressure and temperature in the range of 1 kPa < p < 150 kPa and $0^oC < T < 50^oC$ with an accuracy of 0.1^oC and 20 Pa. Same LED and camera were used for excitation and emission detection during calibration and in experiments described in following sections. Resulting calibration files contain pressure (Psens) and temperature (Tsens) calibration coefficients.

A small shock tube is used to characterise the pressure step response of iPSP. This shock tube uses a 25-100 µm plastic diaphragm between variable diameter driving and driven fluid tubes. The diaphragm is ruptured with the help of a hand-driven plunger needle after the respective fill pressures is reached. Operated with air in both tubes a Mach number of up to 2.5 can be reached. To characterise iPSP driven and driving sections are filled with synthetic air to 6.6 kPa bar and 225 kPa respectively (Mach number = 2.0). A Kulite sensor (XCEL-100-35BARA) and iPSP coated sample are positioned at the end wall of the driven section sustaining a pressure rise of approximately 100 kPa during the maximal measurement time of 4 ms. The results of this tests show a 90% iPSP pressure response to a pressure step after 0.06 ms (t_{90} = 0.06 ms) which is fast enough to resolve expected pressure changes of up to 1000 Hz.

Image Conditioning

During the PSP lifetime measurement multi-exposure images for Gate 1 and Gate 2 are created. For M = 0.9 3000 exposures and for M = 1.05 and M = 1.25 5000 exposures are collected for each gate. Gate 1 and 2 have same exposure times of 20 µs with Gate 1 starting 20 µs before LED flash end and Gate 2 starting with the end of LED flash (±0 µs). Intensity method is used in TSP/iPSP measurements where each image corresponds to one exposure. Raw PSP/TSP images are pre-processed by application of a median 4x4 filter to reduce random noise. According to the respective measurement method ratios of aligned 2D images (*G* = *Gate1/Gate2* and *Gref/Grun* for lifetime or *Iref/Irun* for intensity method) are created and mapped to a 3D mesh. On the 3D model, the calibration is applied resulting in spatial pressure/temperature distribution. In the following step, pressure tap results are compared to PSP results at respective locations. The comparison for each Mach number shows an (approximately equal) offset for each pressure tap. This offset is a systematic error and is caused by different effects e.g. paint degradation, temperature influences. Offset correction is performed applying the mean of PSI-PSP differences to PSP results. Further analyses are performed on the offset corrected 3D images.

Error Analysis

Pressure Systems PSI 8400: The pressure scanner in this system are not temperature compensated leading to a relatively high calculated uncertainty of 0.85% (or 0.879 kPa) full scale output (FSO) [13].

Steady PSP/iPSP: In both cases the analysis is performed after application of calibration and offset correction on a 3D model for corresponding location of each pressure tap. PSP results are evaluated and compared to pressure tap results on the same blade and same test campaign showing a PSI-PSP root mean square (RMS) error of approximately 0.56 kPa. The iPSP coated blade does not feature pressure taps hence the results of the measurements are compared to the results obtained with an uncoated blade equipped with 20 pressure taps (Figure 3) connected to the PSI measurement system. Evaluated at each pressure tap location, the PSI-iPSP RMS error is approximately 1.03 kPa.

Results and Discussion

The results presented in this paper are evaluated for three different isentropic downstream Mach numbers M = 0.9, 1.05 and 1.25. The inlet conditions for all cases are shown in Table 1 and are set to be constant throughout the investigation. This section presents the visualisation of the surface pressure and the quantitative pressure data evaluated at the spanwise pressure tap location. The evaluated pressure is compared with the PSI pressure tap data.

Steady Pressure Sensitive Paint Measurements

For steady pressure measurements one blade was coated with a pressure sensitive paint (PSP), Yorita et al. [14]. The paint parameters are summarised in Table 2. Also shown in Table 2 is the averaged surface roughness of the PSP coat.

Table 2: Steady PSP measurement parameters

Measurement method	Lifetime
PSP Temp. Sensitivity, Tsens	-0.6 %/K
PSP Pressure Sensitivity, Psens	80.4 %/100kPa
Roughness Ra	1.2 µm
Roughness Rz	7.5 µm

In the following figures, the dark regions represent lower pressure and the brighter regions higher pressures. The figures also feature different pressure scales for better visualisation.

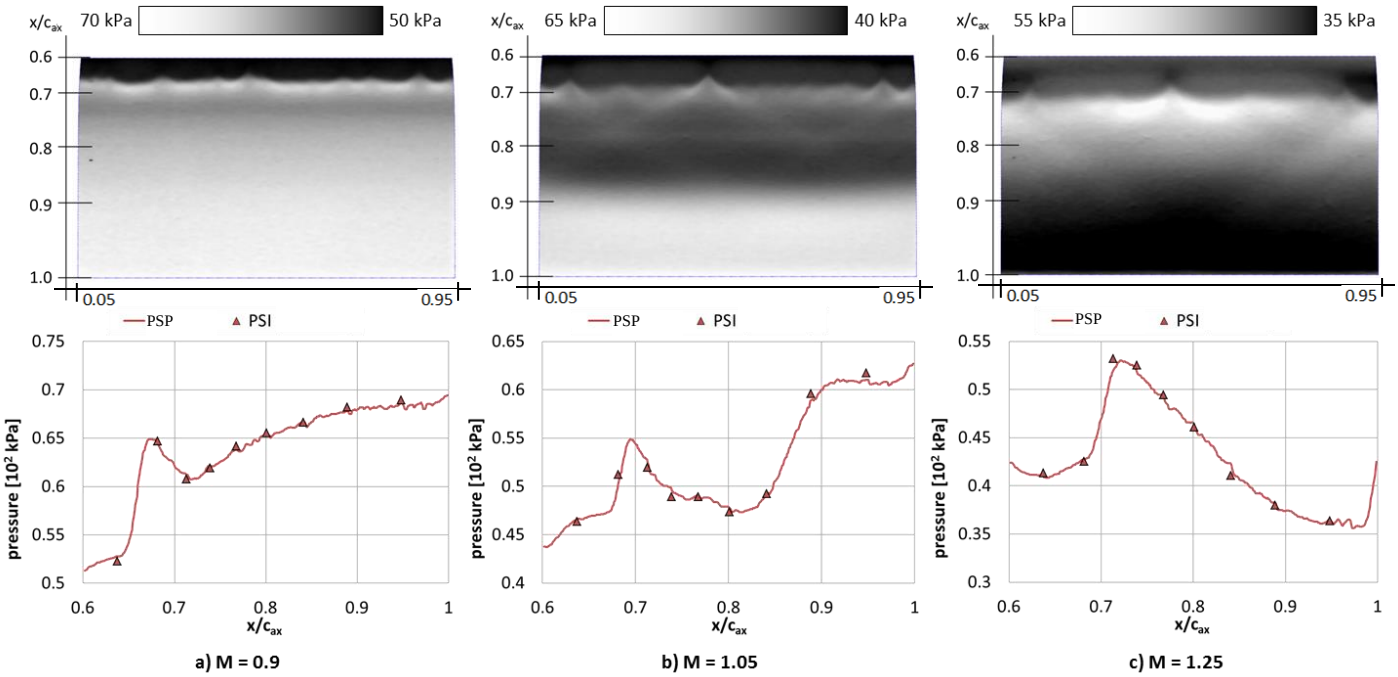

Figure 5: Evaluated PSP results (flow direction from the top down).

M = 0.9

The results of the PSP measurement with the exit Mach number of M = 0.9 are shown in Figure 5a. At this Mach number a dark area of low pressure can be seen between x/c_{ax} = 0.60 and x/c_{ax} = 0.68 (x/c_{ax} - non-dimensionalised axial chord position). Followed by a sharp increase in pressure at x/c_{ax} = 0.68 indicated by a bright spanwise line. This bright line is also seen as a peak value in the quantitative pressure data shown in the Figure 5a at x/c_{ax} = 0.68. The maximum pressure at this position is 65 kPa. After this peak the surface pressure returns to almost 61 kPa and rises slowly until the trailing edge of the guide vane. A comparison with Schlieren images [18], Figure 6a, at this Mach number shows, that the pressure peak is a result of the reattachement of the separation bubble caused by oblique shock. On the surface the separation is characterised by a significant pressure increase at the separation point followed by a pressure plateau and a second pressure increase at the reattachment point. Unfortunately, the region of the separation caused by the oblique shock at this Mach number is not fully captured by this setup. Schlieren images shown in this and following sections are taken in a separate experiment and at a discrete moment during the measurements therefore the positions and features visible might somewhat vary to the time averaged PSP results.

M = 1.05

Figure 5b shows the visualisation of the surface pressure at an isentropic downstream Mach number M = 1.05. At this Mach number two distinct spanwise areas between x/c_{ax} = 0.60 and x/c_{ax} = 0.73 are observed indicating a footprint of the oblique shock wave-boundary layer interaction with separation. Within the grey area (between x/c_{ax} = 0.60 and x/c_{ax} = 0.73), the pressure is almost at a constant value of 47 kPa. This constant pressure is typical for a separated flow and points to a separation bubble at this position. Comparing PSP results with the Schlieren image, Figure 6b, it is observed that the separation is caused by the oblique shock, which is originated from the trailing edge of the upper blade. The peak value detected with PSP at the reattachment at x/c_{ax} = 0.69 is 55 kPa. Unfortunately, there is no pressure tap located at x/c_{ax} = 0.69 to verify this peak value. In spanwise direction, the area of separation is broken by somewhat angular structures near the end walls and near the half span. These structures indicate an interaction of the oblique shock with turbulent wedges at those positions, whereat the majority of the flow interacting with the shock is laminar. As discussed by Babinsky [15], in cases where the laminar- to – turbulent transition occurs upstream of the interaction, the flow structures are significantly affected so that the separation region may disappear completely because of the shock being too weak to separate the boundary layer.

Farther downstream, the darker area indicates a lower surface pressure, where the acceleration of the flow in the guide vane is expected. Between x/c_{ax} = 0.76 to x/c_{ax} = 0.78 instead of the expected continuous decrease the pressure seems to even out. This is caused by the wake of the upper blade reflected oblique shock, which impinges on the surface of the blade at x/c_{ax} = 0.78.

Farther downstream smeared area between x/c_{ax} = 0.82 and x/c_{ax} = 0.91 is observed with the pressure rise from 47.5 kPa to almost 61.0 kPa followed by an area of constant pressure between x/c_{ax} = 0.91 and x/c_{ax} = 0.98. In the Schlieren image [13], Figure 6b, a normal shock is observed at this position. The smeared area between x/c_{ax} = 0.82 and x/c_{ax} = 0.91 is an indicator of unsteady position of the normal shock. At the trailing edge from x/c_{ax} = 0.98 the pressure is

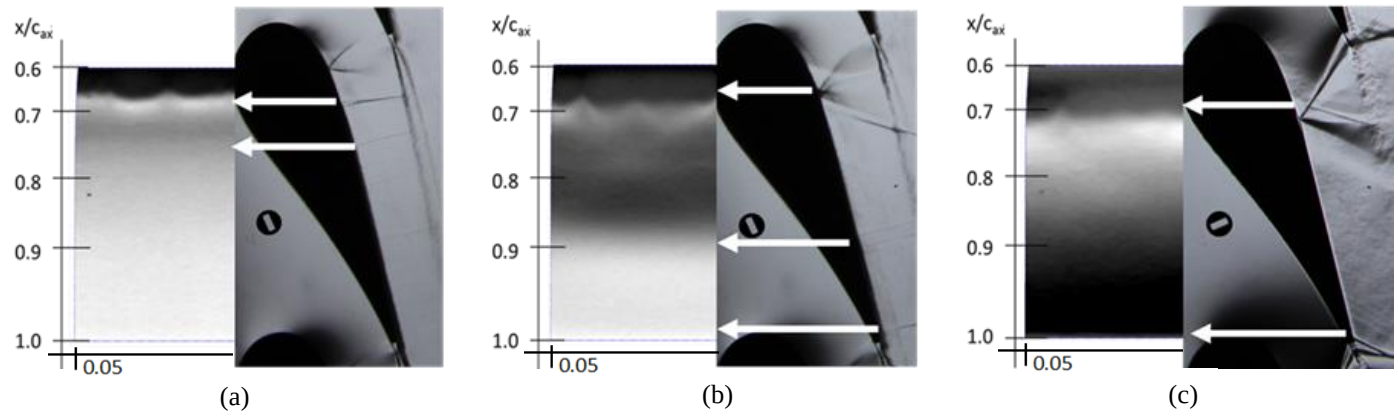

Figure 6: Comparison of PSP surface pressure visualisation and Schlieren images: (a) M = 0.9, (b) M = 1.05, (c) M = 1.25

rising again caused by the suction side leg of the trailing edge shock increasing up to 62.5 kPa, Figure 6b.

M = 1.25

The highest investigated Mach number is M = 1.25. In Figure 5c, similar to M = 1.05, an interaction of the oblique shock with the boundary layer causing a separation bubble is observed between x/c_{ax} = 0.63 and x/c_{ax} = 0.71. This is also seen in the Schlieren images, Figure 6c. The reattachment region features a strong pressure rise from 40 kPa to 52 kPa at x/c_{ax} = 0.71. Analog to M = 1.05 the separation area is divided by triangular patterns in spanwise direction at similar positions. Downstream of the reattachment (between x/c_{ax} = 0.71 and x/c_{ax} = 0.98), the pressure is decreasing to 36 kPa. At the trailing edge (x/c_{ax} = 0.98) a bright line of increasing pressure is observed caused by the suction side leg of the trailing edge shock. The diagonal structures observed between x/c_{ax} = 0.71 and x/c_{ax} = 0.90 are most likely caused by the interaction of the main flow with the secondary flows.

Unsteady Pressure Results from Unsteady (iPSP) Measurements

For steady and unsteady iPSP pressure measurements the surface of one blade is coated with a fast response Pressure Sensitive Paint developed at DLR, Institute for Aerodynamics and Flow Technology. The iPSP coating consists of two layers subsequently applied with a drying period between the applications. The first layer (or basecoat layer) is a mix of particles and a polymer and the second, layer (the active layer) is a mix of luminophore and solvent. The iPSP uses same luminophore as with steady PSP. The characteristics of the paint are summarised in Table 3.

Shock tube tests were carried out to investigate the step response of iPSP and to validate the ability of the paint to resolve expected flow field fluctuations of up to 1000 Hz.

M = 0.9

For this Mach number the camera frame rate was set to 7200 fps with the shutter of 1/fps. In Figure 7 the iPSP measurement at M = 0.9 is evaluated to determine dominant unsteady flow features and frequencies.

Table 3: iPSP measurement parameters

Measurement method	Intensity
Frame rate	Up to 10 000 fps
iPSP temp. sensitivity, Tsens	-2.3 %/K
iPSP pressure sensitivity, Psens	77 %/100kPa
Averaged roughness Ra	2.3 µm
Averaged roughness Rz	10.6 µm

At the position (a) as indicated in Figure 7(I) (time-averaged pressure map) a FFT analysis was performed with the results plotted in Figure 7(II), showing a dominant frequency of 662 Hz. This frequency remains dominant across the whole surface. In Figure 7(III) two periods of the dominant frequency are plotted for a 10 px region as shown in Figure 7(I) displaying a relatively stable position of the reattachment of the separation bubble caused by the oblique shock (b). (The colour map in this image is adjusted to better visualise the flow characteristics.) The dashed arrow (c) indicates a normal shock propagating from the trailing edge upstream to the position of the reattachment (b). Behind the shock (c) an area with periodically increasing and decreasing pressure (d) is observed. In Figure 7(IV) the pressure amplitude of the dominant frequency is plotted highlighting the largest pressure fluctuations in chord direction.

M = 1.05

In Figure 8 the unsteady measurement is evaluated at M = 1.05. The camera frame rate in this and following test was set to 10000 fps with the shutter of 1/s. The dominant frequency in this case is 669 Hz. In Figure 8(III) the position (b) of the oblique shock remains relatively constant and the position (e) of the on the wake of the upper blade reflected shock (b) changes between x/c_{ax} = 0.75 and x/c_{ax} = 0.80. Similar to M = 0.9 a normal shock (c) is running upstream from the trailing edge up to x/c_{ax} = 0.85. The area of periodically increasing and decreasing pressure (d) is also observed at this Mach number. As shown in Figure 8(IV) the major pressure fluctuations occur between x/c_{ax} = 0.85 and x/c_{ax} = 1.00

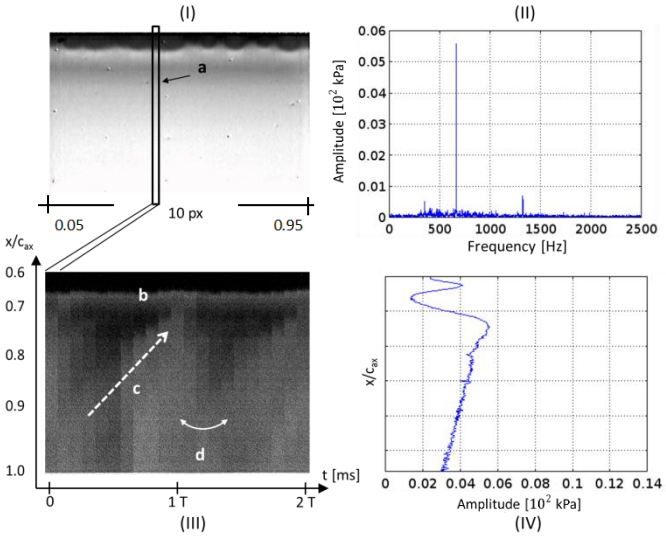

Figure 7: iPSP at M = 0.9

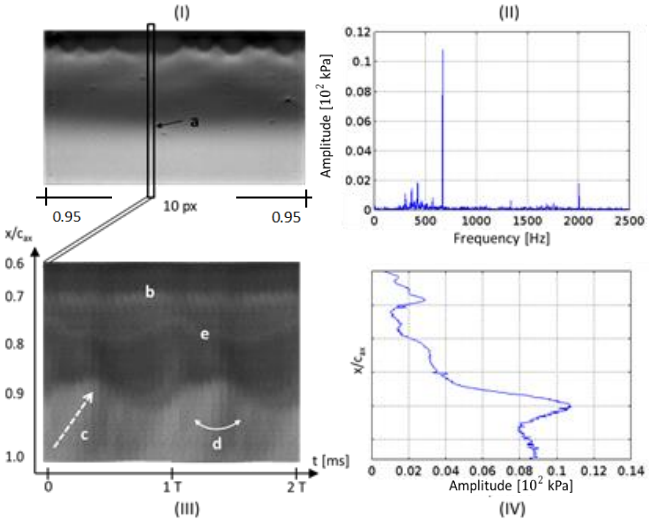

Figure 8: iPSP at M = 1.05

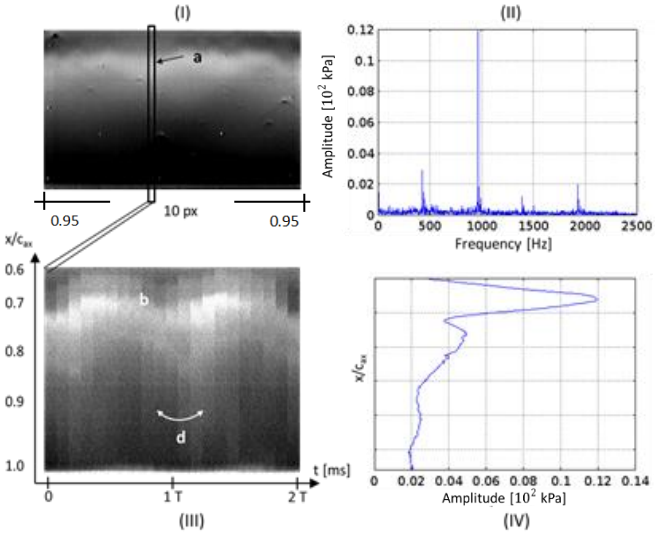

Figure 9: iPSP at M = 1.25

M = 1.25

At this Mach number the oblique shock position (b) in Figure 9(II) shows the highest variation compared to M = 1.05 with a dominant frequency of 966 Hz. Also a normal shock running upstream from the trailing edge, as seen in lower Mach numbers, is absent. Downstream of the oblique shock an area of periodically increasing pressure (d) is visible. The major pressure fluctuations at this Mach number occur between x/c_{ax} = 0.60 and x/c_{ax} = 0.80, Figure 9(IV)

Steady Pressure Results from Unsteady (iPSP) Measurements

The steady state spatial pressures are obtained from unsteady measurement by averaging the images over several periods. The iPSP coated blade does not feature pressure taps so that the results of the measurements are compared to the results obtained with an uncoated blade equipped with 20 pressure taps, Figure 2, connected to PSI measurement system, [13]. For comparison, the steady iPSP pressures as shown in Figure 10 are evaluated at a spanwise position near the position of the pressure taps. In following section, the steady pressures are evaluated exemplary for one Mach number.

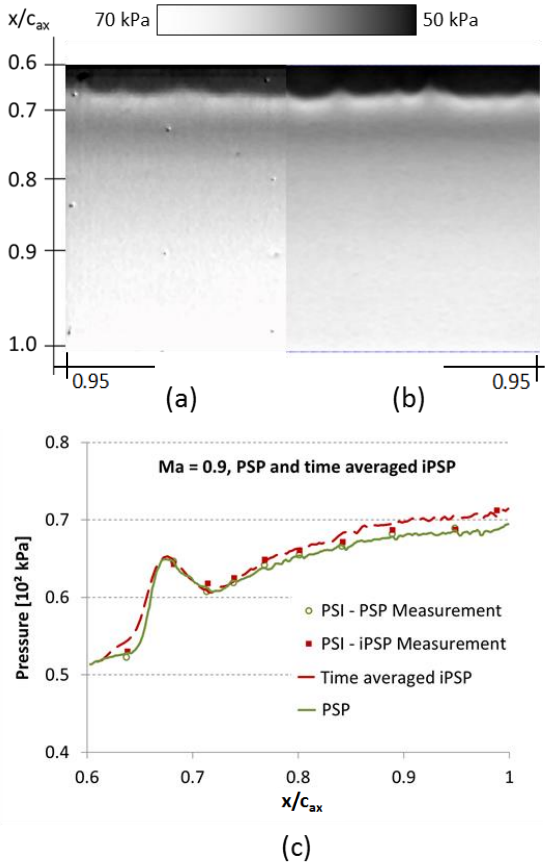

Figure 10: Time averaged iPSP results.

M = 0.9

The result of the steady iPSP evaluation is shown in Figure 10a on the left side. On the right side, the PSP

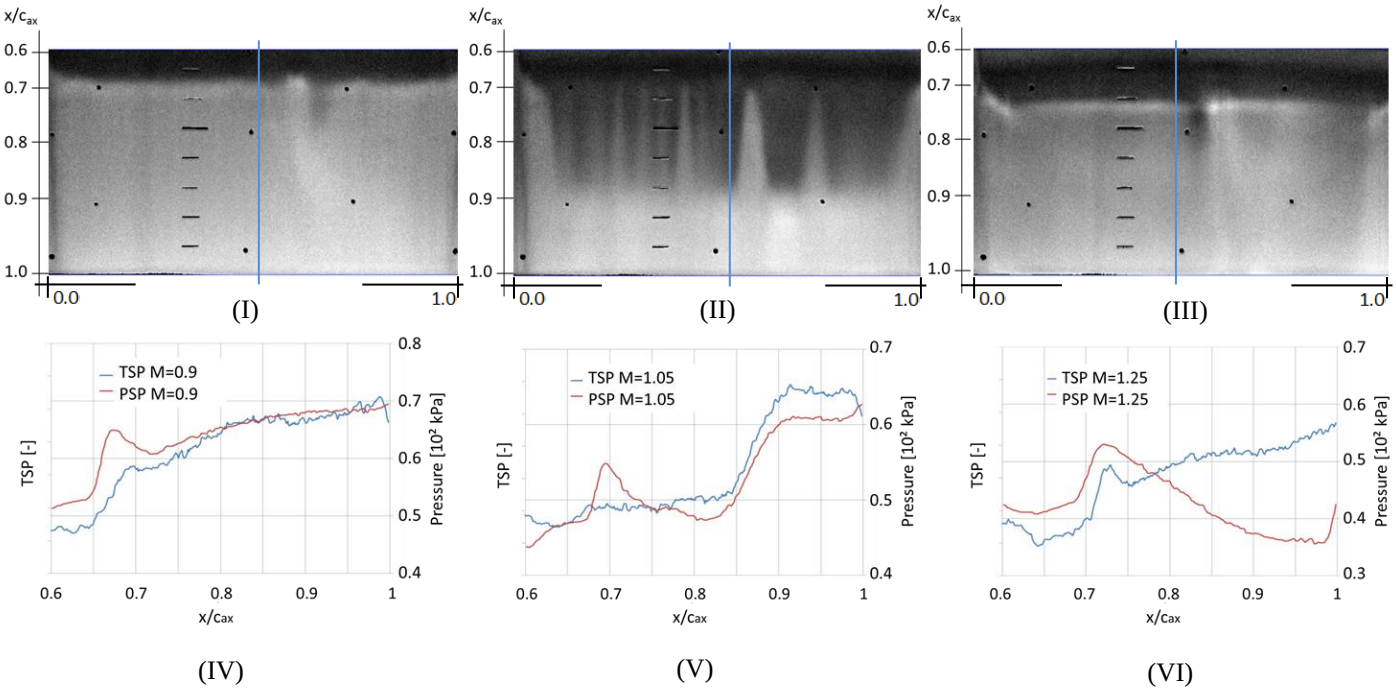

Figure 11: TSP result visualising boundary layer turbulence levels and comparison with PSP measurements.

measurement is shown. The colour map in Figure 10a is adjusted to feature same pressure range. In the Figure 10b pressures of PSP and iPSP are evaluated at a spanwise location near the positon of the pressure taps showing a reasonable agreement.

Temperature Sensitive Paint Measurements

For temperature measurements one blade was coated with a Temperature Sensitive Paint (TSP), Ondrus et al. [16], Table 4. In this section, the qualitative TSP values are compared to quantitative PSP results. The qualitative TSP evaluation is used to visualise laminar to turbulent boundary layer transition. The visualisation is based on different heat transfer coefficients in laminar and turbulent flows resulting in a different response of surface temperature against artificial temperature step. The temperature step is created by switching off the wind tunnel working fluid cooling system generating a gradual positive increase in flow temperature and therefore a temperature difference to the blade surface. Lower heat transfer coefficient inside the laminar boundary layer allows only for a slow increase of surface temperature in contrast to higher heat transfer coefficient inside the turbulent boundary layer and therefore quicker increase of surface temperature. In the TSP images the lower surface temperature is indicated by darker image regions and corresponding higher surface temperature are brighter. The laminar-turbulent transition is indicated by a sudden significant surface temperature increase. The lowest heat transfer coefficient is observed inside separated flow (separation bubble) and is usually indicated by a lowest surface temperature in TSP results. The TSP measurement technique is well described by Fey et al. [17]. In Figures 11 (I, II and III) TSP is evaluated at the midspan (blue line) and plotted in corresponding Figures 11 (IV, V and VI). For comparison, pressure results for matching Mach number are plotted in red.

Table 4: TSP measurement parameters

Measurement method	Intensity
Frame rate	8 fps
TSP temp. sensitivity Tsens	-4 %/K
Averaged roughness Ra	0.05 µm
Averaged roughness Rz	0.3 µm

M = 0.9

As shown in Figure 11(I and IV), at this Mach number the laminar to turbulent transition is triggered by the oblique shock at x/c_{ax} = 0.65 followed by a second relatively strong temperature increase between x/c_{ax} = 0.75 and x/c_{ax} = 0.81 which corresponds with the area of strong pressure fluctuations in iPSP results, Figure 7(IV). Downstream of x/c_{ax} = 0.81 the temperature of the model surface gradually increases toward the trailing edge.

M = 1.05

In Figure 11(V), between x/c_{ax} = 0.6 and x/c_{ax} = 0.68 a low brightness region is observed which corresponds to the constant pressure level of 47 kPa in PSP results. Both effects indicate a separation bubble at this position. In PSP results the separated region is indicated by a pressure plateau [15] and due to a relatively low heat transfer coefficient caused by a low turbulence level in a separation bubble the surface temperature here is also significantly lower. At the reattachment point (x/c_{ax} = 0.68) the surface temperature increases. The increase at reattachment is relatively small indicating that the flow might still be laminar. This is also supported by the decreasing surface pressure after

reattachment and meanwhile almost constant surface temperature up to x/c_{ax} = 0.8. Further, the presence of several turbulence wedges originated from the reattachment region suggest that the general flow reattachment is laminar. From x/c_{ax} = 0.83 a strong increase in pressure and surface temperature occurs. The turbulence level increase highlights laminar to turbulent boundary layer transition triggered by unsteady normal shock. From x/c_{ax} = 0.98 the surface temperature is shown to decrease corresponding to the pressure increase caused by the suction side leg of the trailing edge shock. The decreasing temperature at this position could be an indication of separated flow.

M = 1.25

The comparison of the TSP and PSP for M = 1.25 is shown in Figure 11(VI). Between x/c_{ax} = 0.63 and x/c_{ax} = 0.71 the TSP shows a surface temperature valley caused by the boundary layer separation bubble triggered by the interaction with the oblique shock. At the reattachment point at x/c_{ax} = 0.72 both PSP and TSP feature a peak value. After the peak a second moderate temperature increase between x/c_{ax} = 0.75 and x/c_{ax} = 0.81 is observed which corresponds with the second pressure fluctuation peak in Figure 9(IV) at similar position. The surface temperature increase is followed by a region of relatively constant level between x/c_{ax} = 0.81 and x/c_{ax} = 0.95 followed by another moderate increase, which also corresponds to the third and smallest fluctuation peak in Figure 9(IV). From x/c_{ax} = 0.71 the boundary layer is fully turbulent.

CONCLUSIONS

In this work a series of tests are described carried out using Pressure and Temperature Sensitive Paints for steady measurements, recently developed by the German Aerospace Center (DLR) in Göttingen in corroboration with University Hohenheim. The tests are conducted in a transonic linear cascades at DLR Göttingen (EGG) on a highly loaded turbine guide vane developed within the TFAST research program. Additionally, unsteady measurement using fast response Pressure Sensitive Paint are carried out and the result compared to the steady PSP tests.

This work conclusively shows that the DLR PSP as well as the TSP measurement systems are applicable to provide pressure data on the surface of the guide vanes and to visualise different heat transfer coefficients inside the boundary layer. Boundary layer characteristics and pressure have been visualised at transonic and supersonic Mach numbers. It is shown that the PSP results agree well with the pressure tap data and the visualisation from the Schlieren images.

Unsteady Pressure Sensitive Paint measurements are used to visualise unsteady flow characteristics which, are related to the steady pressure and temperature results.

Findings and conclusions from this work are now used to further improve the TSP/PSP/iPSP measurement techniques for future turbomachinery applications.

NOMENCLATURE

EGG	Transonic Linear Cascade
CCD	Charge-Coupled Device
CMOS	Complementary Metal Oxide Semiconductor
FFT	Fast Fourier Transformation
IR	Infrared
RMS	Root Mean Square
PSP	Pressure Sensitive Paint
TSP	Temperature Sensitive Paint
iPSP	Fast response Pressure Sensitive Paint
A,B	Material coefficients [-]
M	Mach number [-]
T	Temperature [K]
I	Intensity [-]
p	pressure [Pa]
Enr	Activation energy for the non-radioative process [J]
G	Gate image ratio [-]
R	Universal gas constant [J/(K mol)]
τ	Lifetime [s]
t	Pressure recovery time [s]
L	Turbulence level [%]
x	Distance [m]
h	Hight [m]
c	Chord [m]
Ra	Averaged roughness [µm]
Rz	Mean roughness depth [µm]
Fps	Frames per second

Subscripts

ref	Reference
run	Run
in	Inlet
ax	Axial
sens	Sensitivity

ACKNOWLEDGMENTS

Very special thanks go to Dr. Ulrich Henne from the Institute of Aerodynamics and Flow Technology at DLR for his support and expertise during the preparation of this test. Furthermore, with much appreciation, the synthetisation of the paint by Dr. Vladimir Ondrus from University Hohenheim is acknowledged. Our sincerest thanks also go to Dr Jan Martinez Schramm from the Institute of Aerodynamics and Flow Technology at DLR for his support in shock tube tests. Finally yet importantly, many thanks go to Carsten Fuchs at DLR and his expertise in preparation of the model.

REFERENCES

[1] P. Flaszynski, P. Doerffer, R. Szwaba, P. Kaczynski and M. Piotrowicz, "Shock wave boundary layer interaction on suction side of compressor profile in single passage test section," *Journal of Thremal Science, 10.1007/s11630-015-0816-9*, vol. 24, no. 6, pp. 510-515, November 2015.

[2] D. V. Gaitonde, "Progress in shock wave/boundary layer interactions," *Progress in Aerospace Sciences,* vol. 72, pp. 80-99, January 2015.

[3] M. Kameda, "Fast-responding pressure-sensitive paints for unsteady flow measurements," in *10th Pacific Symposium on Flow Visualization and Image Processing*, Naples, Italy, 15-18 June, 2015.

[4] J. W. Gregory, H. Sakaue, T. Liu and J. P. Sullivan, "Fast Pressure-Sensitive Paint for Flow and Acoustic Diagnostics," *Annual Review of Fluid Mechanics,* vol. 46, pp. 303-330, January 2014.

[5] W. Merzkirch, "Techniques of Flow Visualization," Fluid Dynamic Panel of AGARD, ISBN 92-835-0438-0, Paris, December 1984.

[6] W. Bräunling, A. Quast and H.-J. Dietrichs, "Detection of Separation Bubbles by Infrared Images in Transonic Turbine Cascades," *Journal of Turbomachinery*, vol. 110, pp. 504-511, 1988.

[7] W. J. G. Bräunling, Flugzeugtriebwerke: Grundlagen, Aero-Thermodynamik, ideale und reale Kreisprozesse, Thermische Turbomaschinen, Komponenten, Emissionen und Systeme, Springer Vieweg, 10.1007/978-3-642-34539-5, Mai 2015.

[8] T. Liu and J. P. Sullivan, Pressure and Temperature Sensitive Paints, Berlin Heidelberg: Springer-Verlag, 2005.

[9] D. Yorita, U. Henne, C. Klein, V. Ondrus and U. Beifuss, "Improvement of Lifetime-based PSP Technique for Industrial Wind Tunnel Test,," AIAA SciTech 2017, Grapevine, Texas, 2017.

[10] F. Kost and G. Peter-Anton, "Experimental turbine reserch at DLR Göttingen," *Journal of the Gas Turbine Society of Japan*, vol. 32, no. 6, 2004.

[11] C. Kapteijn, J. Amecke and V. Michelassi, "Aerodynamic Performance of a Transonic Turbine Guide Vane with Trailing Edge Coolant Ejection Part I: Experimental Approach," in *ASME 1994 International Gas Turbine and Aeroengine Congress and Exposition, 94-GT-288*, The Hague, June 13-16, 1994.

[12] "TFAST," Transonic Location Effect on Shock Wave Boundary Layer Interaction, 2012. [Online]. Available: http://www.tfast.eu.

[13] A. Petersen, "Basic turbine cascade flow experiment," IB-225-2015-A05, German Aerospace Center (DLR), Göttingen, September 2015.

[14] D. Yorita, C. Klein, U. Henne, V. Ondrus, U. Beifuss and M. Bruse, "Improvement of PtTFPP-based PSP for Lifetime-based Measurement and Application to Transonic Wind Tunnel Test", ISFV16_1129, in *16th International Symposium on Flow Visualization*, Okinawa, Japan, June 24-28, 2014.

[15] H. Babinsky and J. K. Harvey, Shock Wave-Boundary-Layer Interactions, New York, USA: Cambridge University Press, 2011.

[16] V. Ondrus, R. J. Meier, C. Klein, U. Henne, M. Schäferling and U. Beifuss, "Europium 1,3-di(thienyl)propane-1,3-diones with outstanding properties for temperature sensing," *Sensors and Actuators A: Physical,* vol. 233, pp. 434-441, 1 September 2015.

[17] U. Fey, Y. Egami and R. H. Engler, "High Reynolds Number Transition Detection by Means of Temperature Sensitive Paint," in *44th AIAA Aerospace Sciences Meeting and Exhibit*, Reno, Nevada, AIAA-2006-514, 9 - 12 January 2006.

[18] A. Petersen, "Influence of Cooling on the Transition Location in a Straight High Pressure Turbine Cascade," in *Proceedings of 12th European Conference on Turbomachinery Fluid Dynamics & Thermodynamics ETC 12, April 3-7, 2017, ETC2017-155*, Stockholm, Sweden, 2017.